ASSESSING THE POTENTIAL IMPACT OF CLIMATE CHANGE ON RICE YIELD IN THE ARTIBONITE VALLEY OF HAITI USING THE CSM-CERES-RICE MODEL

F. Nicolas, K. W. Migliaccio, G. Hoogenboom,
B. R. Rathinasabapathi, W. R. Eisenstadt

HIGHLIGHTS

- Rice yield decreased in the spring-summer and summer-autumn seasons and increased in the winter-spring season.
- The average annual rice yield in the Artibonite Valley is expected to decrease.
- MarkSim climate data linked with DSSAT provide a means to simulate climate change impacts on crop yield.

ABSTRACT. *Rice (*Oryza sativa*) is one of the major crops in the world and one of the most consumed agricultural products in Haiti, with the main production area in the Artibonite Valley. Crop management, poor soil conditions, and weather uncertainty affect rice production in this region. The objective of this study was to determine the potential impact of climate change on rice yield in the Artibonite Valley of Haiti for future periods (near-term: 2010-2039 and mid-century: 2040-2069) under two Representative Concentration Pathways (RCPs 4.5 and 8.5) defined by the Fifth Assessment Report of the Intergovernmental Panel on Climate Change (IPCC). The Crop Estimation Resource and Environment Synthesis (CERES)-Rice model of the Decision Support for Agrotechnology Transfer (DSSAT) cropping system model was used to perform the simulations using local soil characteristics, meteorological data, and crop management following model calibration with local experimental data. Temperature (maximum and minimum) was predicted to increase during all three rice-growing seasons (spring-summer, summer-autumn, and winter-spring). Under both RCPs (4.5 and 8.5), the simulation results indicated that the ensemble-mean rice yield decreased during the spring-summer and summer-autumn seasons (by 5.1% to 6.6% and by 5.4% to 8.3%, respectively) and increased during the winter-spring season (by 2.3% to 3.6%). Although yield increased during the winter-spring season, the average annual yield was predicted to decrease by 3.6% to 7.1% and by 4.2% to 9.6% for the near-term and mid-century climate periods, respectively. These findings could assist with the implementation of adaptation strategies to mitigate the projected negative impact of climate change on rice production in Haiti.*

Keywords*. Cropping system model, DSSAT, Food security, Global climate model, Rice production, Systems analysis.*

The increase of greenhouse gases (GHG) such as carbon dioxide (CO_2), methane (CH_4), and nitrous oxide (N_2O) due to anthropogenic actions has led to climate change, with worldwide economic and environmental implications. Climate change has impacted the cyclic pattern of weather conditions and has triggered an increase in temperature, an increase in the frequency of extreme weather events, and a decrease in precipitation for many locations across the globe (Pachauri et al., 2014; Pranuthi and Tripathi, 2018). The Fifth Assessment Report (AR5) of the Intergovernmental Panel on Climate Change (IPCC, 2014) states that precipitation will likely change depending on the region, and the global mean temperature could rise by 4.8°C by the end of the 21st century. These climate changes have been predicted to be much more detrimental to developing countries such as Haiti compared to more developed countries.

Extreme weather events coupled with a temperature increase and precipitation decrease are predicted to have a negative impact on agricultural productivity, as crop production systems are sensitive to the changes in local weather conditions (IPCC, 2014). An increase in the mean seasonal temperature could lead to a reduction in crop growth periods, resulting in a decrease in final yield (Bhattacharya, 2019; Petersen, 2019; van Oort and Zwart, 2017), and permanent alteration of ecosystems may affect water availability. In Haiti, both the social and natural systems are already affected by climate change, and increasing weather fluctuation will affect the livelihoods of those near poverty who heavily depend on natural resources (Singh and Cohen, 2014). The

Submitted for review in January 2020 as manuscript number NRES 13868; approved for publication as a Research Article by the Natural Resources & Environmental Systems Community of ASABE in June 2020.

The authors are **Floyid Nicolas,** Graduate Student, **Kati W. Migliaccio,** Professor, and **Gerrit Hoogenboom,** Preeminent Scholar, Department of Agricultural and Biological Engineering, **Bala R. Rathinasabapathi,** Professor, Department of Horticultural Sciences, and **William R. Eisenstadt,** Professor, Department of Electrical and Computer Engineering, University of Florida, Gainesville, Florida. **Corresponding author:** Kati W. Migliaccio, P.O. Box 110570, 1741 Museum Road, Gainesville, FL 32611-0570; phone: 352-294-6743; e-mail: klwhite@ufl.edu.

  ISSN 2151-0032 https://doi.org/10.13031/trans.13868

Haitian Ministry of Agriculture, Natural Resources, and Rural Development (Ministère de l'Agriculture, des Ressources Naturelles, et de Développement Rural, or MARNDR) has observed an increase in temperature of 1°C from 1973 to 2003. According to Singh and Cohen (2014), Haitian farmers are struggling to adapt their practices to changing weather conditions due to lack of an efficient climate monitoring network and appropriate information delivery systems.

More than 60% of Haitians are employed in the agricultural sector and depend entirely on agriculture for their income and livelihood. Due to climate events such as drought, floods, and storms, Haiti's crop production has been severely impacted, causing a reduction in crop yield and an increase in food insecurity (Singh and Cohen, 2014). Since 1960, the average annual precipitation has decreased by 5 mm per month per decade, and the frequency of hot days and nights has increased from 48 to 63 days between 1960 and 2003 (USAID, 2017). The unpredictable rainfall and the season shift challenge current agricultural management practices, such as planting dates. Extreme weather events have impacted the already weak agrarian infrastructure. Climate change will likely exacerbate these conditions.

Many researchers have investigated the potential effects of the changing climate on agricultural production on global and regional scales (Challinor et al., 2014; Dixit et al., 2018; Petersen, 2019; Reilly et al., 2003; Tubiello et al., 2002; Xiong et al., 2008). They found that crop production would negatively be affected in some regions, while the changing climate might be beneficial to crop production in other locations. Only a few studies (ME, 2013; USAID, 2011, 2013, 2017) have focused on predicting the potential impact of climate change in Haiti, and those studies indicate that the change in the climate factors is expected to exacerbate the living conditions and could have a severe impact on Haitian agriculture. However, those studies were conducted on a national scale, with no regard for regional or local assessment, and the authors did not evaluate the impact of the changing climate on crop yield. Those simulations also did not consider the local soil nor the commonly grown crop cultivars. Therefore, the potential effects of climate change on crop production remain unclear in the Artibonite Valley in Haiti. Based on previous climate change studies (Pranuthi and Tripathi, 2018; Tiepolo and Bacci, 2017; USAID, 2011) and the AR5 (IPCC, 2014), this study hypothesizes that climate change will reduce rice yield in the Artibonite Valley. The objectives of this study were, therefore, to simulate, on a seasonal basis, the future climate trend for the near-term (2010-2049) and mid-century (2050-2069) climate periods under RCP 4.5 and RCP 8.5 and to evaluate the potential impact of these future climate trends on rice yield in the Artibonite Valley.

Materials and Methods

Study Site

The study was conducted in the Artibonite Valley, which is located between 18° 50′ and 19° 18′ N and between 72° 37′ and 72° 00′ W in Haiti (fig. 1). Rice is cultivated on over 35,000 ha in the valley under flooded conditions for all growing seasons. About 18,000 ha is cultivated during the rainy season due to the unavailability of water in these locations during the dry season. Approximately 60 km of streams cross the regions, and the water distribution and irrigation infrastructures are operated by the Organization for the Development of the Artibonite Valley (ODVA), one of the largest operating bodies of the Haitian Ministry of Agriculture (Wilcock and Jean-Pierre, 2012).

The maximum temperature ranges from 29.0°C in December to 34.3°C in July, and the minimum temperature varies between 17.8°C in January and 19.9°C in July. The average annual temperature is 27°C, and the average relative humidity is 63% in April and 69% in September. There is a rainy season from May to October, which receives 500 to 1200 mm of rain, and a dry season from November to April, which receives 50 to 100 mm of rain (Lamy et al., 2011). However, Lamy et al. (2011) did not provide the period of record from which these averages were obtained.

The NASA Prediction of Worldwide Energy Resources (POWER) project provides weather data starting from 1981 (https://power.larc.nasa.gov). We used NASA POWER to estimate the average temperature in the Artibonite Valley from 1981 to 2017. The average maximum temperatures in the location were 29.6°C in December and 34.0°C in July, and the minimum temperatures varied from 19°C in December to 23.8°C in August. These results are similar to the values reported by Lamy et al. (2011).

Rice is grown in all ten provinces of Haiti. However, over 70% of Haitian rice is produced in the Artibonite Valley. Of the remaining rice production in Haiti, 15% is cultivated in the northern region of the country, while the rest is cultivated in the southwestern region. The total rice production area in the Artibonite Valley is over 50,000 ha, with some of this area cultivated only during the rainy season due to lack of water for irrigation during the dry season (Wilcock and Jean-Pierre, 2012). The crop is cultivated mostly under flooded conditions or under irrigation during all three growing seasons, which include spring-summer, summer-autumn, and winter-spring. Six rice varieties are commonly grown in the valley, including Malaïka, Schela, Bogapoté, Tididi, CAP, and TCS10. Varieties such as Schela are grown for their culinary quality, and varieties such as TCS10 are widely produced because of their high potential yield (FEWS NET, 2018).

DSSAT CSM-CERES-Rice

The DSSAT cropping system model (CSM) is a process-based dynamic simulation model (Hoogenboom et al., 2019; Jones et al., 2003). The CSM-CERES-Rice model of DSSAT version 4.7 (Hoogenboom et al., 2018) was used in this study. The optimal range of temperature considered in the CSM-CERES-Rice model is between 14°C and 32°C (Lamsal et al., 2013). Outside of this temperature range, yield decreases. The model simulates daily phenological development and biomass production in response to local weather and soil conditions and crop management practices (Ritchie et al., 1998). The input data files required by DSSAT are weather (minimum temperature, maximum temperature, rainfall, solar radiation), soil (soil type, organic

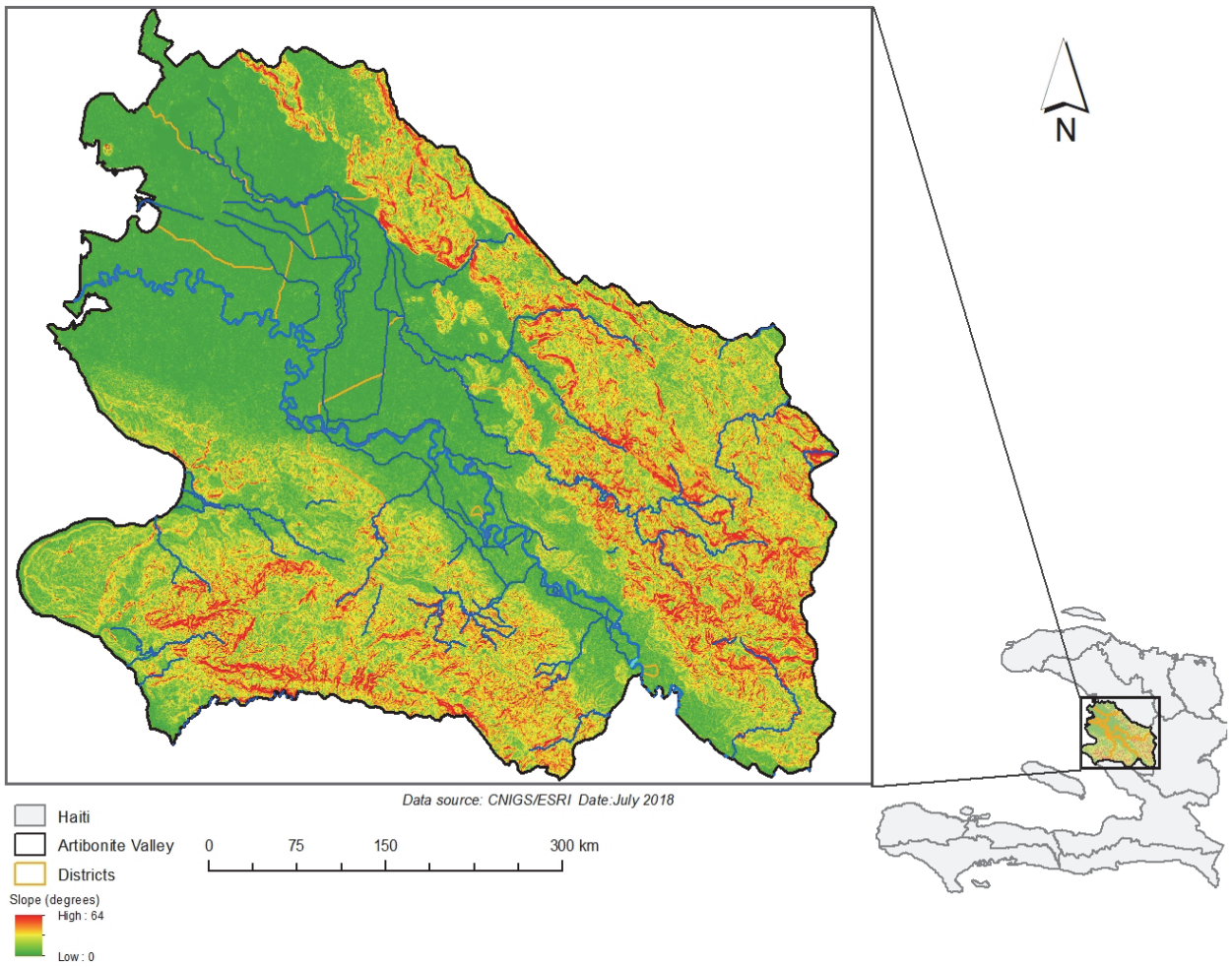

Figure 1. The main region for rice production in the Artibonite Valley, Haiti.

matter, texture, electrical conductivity, etc.), genotype characteristics (cultivar), and management practices (transplanting date, row and plant spacing, sowing depth, nitrogen fertilizer application rates and dates, irrigation application rates and dates) (Hoogenboom et al., 2012).

CSM-CERES-Rice has been well tested for various types of environments and is able to sufficiently simulate rice growth, development, and yield for various climate conditions and genetic variations (Vaghefi et al., 2013). The model has been used to forecast maturity and yield for both weather variability and changing climate in many regions of the world, including North and South America, Europe, Africa, and Asia (Dass et al., 2012; Kontgis et al., 2019; Singh et al., 2014, 2016). CSM-CERES-Rice and EPIC are reported as the most commonly used models in climate change studies (White et al., 2011). CSM-CERES-Rice includes soil organic matter decomposition routing and routines describing the relevant crop management, and the model has been able to evaluate the effect of changes in temperature and atmospheric CO_2 concentration on rice yield and CH_4 emissions (Vaghefi et al., 2013). In the model, the development stages are controlled by the growing degree days (GDD). The different growth stages, including juvenile, floral, heading, flowering, grain filling, maturity, and harvest, correspond to a certain value of cumulated GDD. The GDD is therefore important to rice growth and development and ultimately yield. More details about GDD are provided by Yan et al. (2006). In CSM-CERES-Rice, the crop reaches the highest production when the temperature is between the baseline and the optimal. However, rice growth and yield decline when the temperature is either extremely high or very low (Guo et al., 2019).

Weather Data for Model Input

In Haiti, the availability of daily weather data from weather stations is limited, and such data were not available for this study area. Satellites are an alternative source of weather data, although they have inherent uncertainties. For locations with limited measured data, gridded weather data can be used to obtain the data needed for crop simulation models (Battisti et al., 2018; White et al., 2008). Bai et al. (2010) used NASA POWER satellite solar radiation data and ground station data to simulate potential corn yield in China. They concluded that the solar radiation data from NASA POWER was a viable option for a regional and national crop simulation model.

The NASA POWER satellite weather system (https://power.larc.nasa.gov) was developed to provide meteorological data for direct applications in fields such as architecture,

energy, and agrometeorology. Weather information is derived from gridded data systems and directly from multiple data sources (Maldonado et al., 2019). Weather data from the latest version of NASA POWER (Release 8) are available on a global grid with a spatial resolution of 0.5° latitude by 0.5° longitude (Stackhouse et al., 2018). Kontgis et al. (2019) used NASA POWER to calibrate the CSM-CERES-Rice model for the Mekong River delta in Vietnam because no on-site weather data were available. Therefore, in this study, NASA POWER daily rainfall, temperature (maximum and minimum), and solar radiation data were used for calibration of the model for the Artibonite Valley of Haiti.

FIELD EXPERIMENTS

Three years of rice crop data, including management practices, phenology, and yield for two varieties (TCS10 and CAP), were provided by the Haitian Ministry of Agriculture. The field experiments had been conducted to identify a fertilizer recommendation for rice farmers in the Artibonite Valley. The results included the responses of different varieties, including CAP and TCS10, to different nitrogen fertilizer application rates (0, 30, 50, 70, 75, 90, 100, 120, and 150 kg N ha^{-1}). The pre-germinated seeds were sown in shallow furrows, and the seeds were covered with a thin layer of soil. The length of stay of seedlings in the nursery was 22 to 25 days. Prior to the field experiments, the field was plowed and harrowed with a tiller.

The two-variety experiments performed by the Ministry of Agriculture were conducted in a randomized block design at an experimental farm (Mauger) in the Artibonite Valley. The first experiment was conducted during the winter-spring season of 2012 and had three blocks and four treatments (0, 50, 75, and 100 kg N ha^{-1}). Each experimental unit was subdivided into two subunits in which the two rice cultivars (TCS10 and CAP) were assigned (table 1). The second experiment had four blocks and six treatments (25, 50, 75, 100, 125, and 150 kg N ha^{-1}) and was conducted during the summer-autumn season of 2014 with only cultivar TCS10. The third experiment was conducted with cultivar TCS10 during the spring-autumn summer of 2015 and included three blocks with four treatments in each block. Two experiments were conducted with the CAP cultivar alone (table 1). The first experiment was conducted during the autumn-winter season of 2012 in three blocks with four treatments (30, 60, 90, and 120 kg N ha^{-1}). The second experiment was conducted during the spring-summer season (2016) in three blocks, with seven treatments per block.

SOIL DATA

A soil survey conducted in the Artibonite Valley showed that the valley is relatively homogeneous and generally has sandy loam soils with an average of 29% sand, 30% silt, and 41% clay for the top 30 cm of the soil profile and 29% sand, 31% silt, and 40% clay for the second layer at a depth of 30 to 60 cm. These soils are neutral to slightly alkaline, with a pH between 7.2 and 8.0 for the top layer and between 7.3 and 8.2 for the second layer. This alkalinity is due to the accumulation of calcareous alluvium that forms the soils of the valley. In the top 30 cm, the average organic matter content is 1.7%, the electrical conductivity is 0.54 mmhos cm^{-1}, the average nitrogen content is 6.75 t ha^{-1}, the average assimilable phosphorus content is 0.050 t ha^{-1}, and the average potassium content is

Table 1. Input parameters for management practices of the TCS10 cultivar for the CSM-CERES-Rice model. The data were obtained from field experiments conducted in the Artibonite Valley by the Haitian Ministry of Agriculture.

Treatment (kg N ha^{-1})	Transplanting Date (and Growing Season)	Cultivar	Application Date (AT = after transplanting) and Proportion of Fertilizer (Urea) Applied			Harvesting Date
			20 days AT	31 days AT	62 days AT	
0	16 Feb. 2012 (winter-spring)	TCS10 and CAP	0%	0%	0%	3 June 2012
50			30%	40%	30%	
75			30%	40%	30%	
100			30%	40%	30%	
	30 July 2014 (summer-autumn)	TCS10	15 days AT	30 days AT	61 days AT	29 Nov. 2014
25			30%	40%	30%	
50			30%	40%	30%	
75			30%	40%	30%	
100			30%	40%	30%	
125			30%	40%	30%	
150			30%	40%	30%	
	13 May 2015 (spring-summer)	TCS10	30 days AT	45 days AT	58 days AT	17 Sept. 2015
30			30%	40%	30%	
60			30%	40%	30%	
90			30%	40%	30%	
120			30%	40%	30%	
	24 Sept. 2012 (autumn-winter)	CAP	28 days AT	42 days AT	56 days AT	3 Dec. 2013
30			30%	40%	30%	
60			30%	40%	30%	
90			30%	40%	30%	
120			30%	40%	30%	
	14 May 2016 (spring-summer)	CAP	28 days AT	42 days AT	56 days AT	30 Sept. 2016
0			0%	0%	0%	
25			30%	40%	30%	
50			30%	30%	30%	
75			30%	40%	30%	
100			30%	40%	30%	
125			30%	40%	30%	
150			30%	40%	30%	

Table 2. Soil data for the Mauger farm in the Artibonite Valley (EC = electrical conductivity, K = potassium, CEC = cation-exchange capacity, N = nitrogen, P = phosphorus, OC = organic carbon, and OM = organic matter).

Soil Profile	pH (H_2O)	EC (mmhos cm^{-1})	K (cmol kg^{-1})	CEC (cmol kg^{-1})	N (%)	P (ppm)	OC (%)	OM (%)	Clay (%)	Silt (%)
0 to 30 cm	8.2	0.364	0.27	23	0.19	0.14	1.71	2.94	41	30.2
30 to 60 cm	8.28	0.322	0.32	22.2	0.14	11.5	1.06	1.82	39.8	31.1

0.42 t ha^{-1}. In the second layer, the average organic matter content is 1.4%, the electrical conductivity is 0.60 mmhos cm^{-1}, the average nitrogen content is 4.172 t ha^{-1}, the average assimilable phosphorus is 0.058 t ha^{-1}, and the average potassium content is 0.421 t ha^{-1} (Louissaint and Duvivier, 2003). Lamy et al. (2011) performed soil analysis at the Mauger farm, where the field experiments were conducted, and reported data for the two layers (0 to 30 cm and 30 to 60 cm), as shown in table 2.

Model Calibration and Evaluation

The data used for model calibration and evaluation were obtained from the field experiments conducted by the Haitian Ministry of Agriculture, as described previously. The field experiments were conducted under flooded conditions with different levels of nitrogen fertilizer application. Model calibration was performed by adjusting the cultivar coefficients to reduce the difference between simulated and observed values of phenology, biomass, and yield. The genetic parameters included the phenological (P1, P2O, P2R, P5) and growth (G1, G2, G3, G4) coefficients (table 3). Two years of data (2012 and 2014 for cultivar TCS10; 2012 (winter-summer season) and 2012 (autumn-winter season) for cultivar CAP) on rice yield, phenology, and management practices were used to estimate the genetic parameters. The second experiment with the CAP cultivar ended in winter 2013. One year of data (2015 for TCS10; 2016 for CAP) was used for model evaluation.

The model for TCS10 was calibrated with two fertilizer treatments (100 and 150 kg N ha^{-1}) with the highest nitrogen application and without water stress from two different experiments (2012 and 2014, respectively). The first experiment was conducted during winter-spring 2012, and the second experiment was conducted during summer-autumn 2014. The model evaluation was then performed using the 120 kg N ha^{-1} fertilizer treatment with no water stress from the experiment conducted in spring-summer 2015.

The model for CAP was calibrated with both the 100 kg N ha^{-1} fertilizer treatment in the winter-spring season of 2012 and the 120 kg N ha^{-1} fertilizer treatment in the autumn-winter season of 2012. These two treatments were free of water stress and were the highest nitrogen amounts applied in their respective seasons. The model was evaluated using the 150 kg N ha^{-1} fertilizer treatment with no water stress from the spring-summer season of 2016.

Using the generalized likelihood uncertainty estimation (GLUE) method (Beven and Binley, 1992), the phenological coefficients were estimated with the anthesis and harvest maturity dates, while the growth coefficients were estimated with the final yield and yield components. The GLUE method is a Bayesian Monte Carlo technique that has been widely used for model parameter estimation (He et al., 2010; Rankinen et al., 2006) and is suitable for highly parameterized models (Sun et al., 2016). DSSAT includes a GLUE tool for estimating the cultivar coefficients (Buddhaboon et al., 2018; Jones et al., 2011). The GLUE tool was run 30,000 times to estimate the genetic parameters during the calibration process (Gao et al., 2020). The generated coefficients were then used to simulate the experimental results and assess the difference between the observed and predicted phenology and growth values. When the results showed a suitable agreement between the predicted and observed values, the evaluation was performed.

The evaluation was conducted by running the model with the treatments that were not used in the calibration process. The root mean square error (RMSE) and the normal root mean square error (NRMSE) were the goodness-of-fit indicators used to evaluate the model performance by estimating the errors between the simulated and observed values for the flowering and maturity dates and final yield (Yang et al., 2014):

$$\mathrm{RMSE} = \left[\frac{1}{n} \sum_{i=1}^{n} \left(S_i - O_i \right)^2 \right]^{1/2} \quad (1)$$

$$\mathrm{NRMSE}\ (\%) = \frac{\mathrm{RMSE}}{\bar{O}_i} \times 100 \quad (2)$$

Table 3. Description and values of the phenological (P) and growth (G) coefficients for rice cultivars TCS10 and CAP (widely cultivated in the Artibonite Valley of Haiti) for the CSM-CERES-Rice model after calibration with GLUE.

Coefficient	Definition	TCS10	CAP
P1	Period expressed as growing degree-days (GDD) above a base temperature of 9°C in the basic vegetative phase of the plant	475.1	638.9
P20	The critical photoperiod or longest day length (in hours) during which development occurs at a maximum rate	175.3	195.2
P2R	The extent to which phasic development leading to panicle initiation is delayed (expressed as GDD in °C) for each hour increase in photoperiod above P2O	375.5	373.6
P5	The time period (GDD) from the beginning of grain filling to physiological maturity with a base temperature of 9°C in the grain filling phase	11.1	12.2
G1	The coefficient for the potential number of spikelets per panicle	46.3	48.4
G2	The single-grain weight under ideal growing conditions (non-limiting light, water, nutrients and absence of pests and diseases)	0.025	0.025
G3	The tillering coefficient relative to IR64 cultivars	0.90	0.82
G4	The temperature tolerance coefficient	1.00	0.93

where S_i and O_i are the predicted and observed parameter values, respectively, n is the number of observations, $\bar{O}_i$ is the observed mean value, and i is each observation. A simulation is considered excellent when the NRMSE is less than 10%, good with an NRMSE between 10% and 20%, fair with an NRMSE between 20% and 30%, and poor if the NRMSE is higher than 30% (Rinaldi et al., 2003).

CLIMATE DATA

The MarkSim DSSAT weather file generator (http://gismap.ciat.cgiar.org/MarkSimGCM/) was used to generate climate data for five global climate models (GFDL-ESM2M, HadGEM2-ES, IPSL-CM5A-LR, MIROC-ESM-CHEM, and NorESM1-M) that were selected for RCP 4.5 and RCP 8.5 (table 4). These five GCMs are from Phase 5 of the Coupled Model Intercomparison Project (CMIP5) and were the only models to be bias-corrected and downscaled by the Inter-Sectoral Impact Model Intercomparison (ISI-MIP) (Li et al., 2016; Warszawski et al., 2014). Therefore, these GCMs were suitable for use in this study. The MarkSim tool was developed to generate weather data for Latin America and Africa. The weather generator includes climate data from more than 9,200 stations around the world. The MarkSim weather generator is based on a third-order Markov process that considers events that occurred over the previous three days. Climate data (solar radiation, minimum and maximum temperatures, and rainfall) for 1980 to 2009 were downloaded from MarkSim for use as a baseline (Jones and Thornton, 2000). Climate data (solar radiation, minimum and maximum temperatures, and rainfall) for future periods under RCP 4.5 and RCP 8.5 were also downloaded from MarkSim. Data for 2010 to 2039 were used for the near-term period, and data for 2040 to 2069 were used for the mid-century period. The CO_2 concentration levels (baseline CO_2 = 360 ppm, RCP 4.5 near-term CO_2 = 423 ppm, RCP 4.5 mid-century CO_2 = 499 ppm, RCP 8.5 near-term CO_2 = 432 ppm, and RCP 8.5 mid-century CO_2 = 571 ppm) were obtained from the Agricultural Model Intercomparison and Improvement Project (AgMIP; www.AgMIP.org) (Rosenzweig et al., 2018).

MODEL SCENARIO SIMULATIONS

In an agricultural system, numerous ecophysiological processes are influenced by environmental conditions (CO_2 concentration, temperature, and rainfall) and management factors (nutrients and irrigation). For the climate simulations in this study, factors such as cultivar, nitrogen fertilizer applications, soil water content, and soil conditions remained constant, while temperature, rainfall, solar radiation, and CO_2 concentrations were considered independent variables. The temperature, rainfall, and solar radiation varied daily. The CO_2 concentrations were fixed for each 30-year period but varied for historical and future periods and for different RCPs. The MarkSim climate data were organized and imported into DSSAT. The CO_2 concentrations from AgMIP were added in the environmental section of the DSSAT seasonal crop management files. With the cultivars, climate data, and soil data configured, the model simulated the potential impact of climate change on rice yield under RCP 4.5 and RCP 8.5 for the region of study.

Rice farmers in the Artibonite Valley plant three rice seasons, i.e., spring-summer, summer-autumn, and winter-spring (table 5). Most of the farmers transplant rice in the first week of April for the spring-summer season, in mid-August for the summer-autumn season, and in the first week of December for the winter-spring season (FEWS NET, 2018). Therefore, April 15, August 22, and December 1 were used as planting dates for the spring-summer, summer-autumn, and winter-spring seasons, respectively. The harvesting dates were defined to be at harvest maturity and were simulated and predicted by the model.

The phenology and yield of both cultivars were simulated for all seasons for the baseline, near-term, and mid-century climate periods under both RCP 4.5 and RCP 8.5. The effect of climate change on rice growth stages (anthesis and physiological maturity) and yield were assessed by comparing the simulations of the two periods (near-term and mid-century) under both RCPs to the simulations obtained for the baseline. The variables of interest (duration to anthesis, duration to maturity, and yield) were evaluated with each of the five GCMs over 30 years for each climate period.

RESULTS AND DISCUSSION

MODEL CALIBRATION AND EVALUATION

DSSAT version 4.7.1 was used to investigate the climate change impact on rice yield in the Artibonite Valley. For the calibration of cultivar TCS10, the RMSE for yield was 193.4 kg ha^{-1}, and there was no difference between the simulated and observed anthesis dates (80 days after planting) and physiological maturity dates (108 days after planting). For model evaluation, there was a one-day difference in the

Table 4. Information related to the five global climate models (GCMs) used in this study.

GCM	Model Source	Reference
GFDL-ESM2M	NOAA Geophysical Fluid Dynamics Laboratory, U.S.	Dunne et al., 2012
HadGEM2-ES	Met Office Hadley Center, U.K.	Collins et al., 2008
IPSL-CM5A-LR	L'Institut Pierre-Simon Laplace, France	Dufresne et al., 2013
MIROC-ESM-CHEM	Japan Agency for Marine-Earth Science and Technology, Atmosphere, and Ocean Research of the University of Tokyo and National Institute for Environmental Studies	Watanabe et al., 2011
NorESM1-M	Norwegian Climate Center	Iversen et al., 2013

Table 5. Current planting and harvesting dates for the Artibonite Valley. These planting dates were simulated in the DSSAT seasonal tool to evaluate the potential impact of climate change on rice yield for each growing rice season (P = planting period; H = harvesting period).

Season	Jan.	Feb.	March	April	May	June	July	Aug.	Sept.	Oct.	Nov.	Dec.
Spring-summer	-	-	-	P	-	-	H	-	-	-	-	-
Summer-autumn	-	-	-	-	-	-	-	P	-	-	H	-
Winter-spring	-	-	H	-	-	-	-	-	-	-	-	P

flowering dates (81 days observed vs. 80 days simulated) and no difference in the maturity dates (106 days after planting). The RMSE for the TCS10 evaluation yield was 144 kg ha^{-1}.

The calibration results for CAP showed no difference between the simulated and observed flowering dates (78 days after planting), and the simulated maturity dates were one day later than observed (107 days simulated vs. 108 days observed). The RMSE was 505.8 kg ha^{-1} for the CAP calibration yield. The model evaluation showed no difference in the anthesis dates (80 days after planting), one day difference for the maturity dates (108 days simulated vs. 107 days observed), and the RMSE was 210 kg ha^{-1} for the CAP evaluation yield.

The rice production in the Artibonite Valley simulated by CSM-CERES-Rice showed good agreement with the measured data for cultivars TCS10 and CAP. The NRMSE values for cultivar TCS10 were 1%, 1%, and 2% for the anthesis and maturity dates and yield, respectively, while the NRMSE values for cultivar CAP were 1%, 1%, and 3% for the same variables. The NRMSE values for all parameters were less than 10% (Jamieson et al., 1991; Rinaldi et al., 2003); hence, the performance of the model was considered excellent (table 6). Figure 2 shows the relationship between the simulated and observed rice grain yields for cultivars TCS10 and CAP in the Artibonite Valley of Haiti.

Future Climate Scenarios

The future climate scenarios were evaluated with respect to changes in the minimum and maximum temperatures, solar radiation, and rainfall for each rice growing season. The minimum and maximum temperatures both increased for all GCMs for all growing seasons for the near-term and mid-century climate periods under both RCP 4.5 and RCP 8.5 compared to the baseline (fig. 3).

Under RCP 4.5, the ensemble-mean maximum temperature for the spring-summer season increased by 1.2°C to 1.6°C for the near-term and by 1.7°C to 2.3°C for mid-century, while for the summer-autumn season it increased by 1.6°C to 2.0°C for the near-term and by 2.0°C to 2.8°C for mid-century. For the winter-spring season, the ensemble-mean maximum temperature increased by 0.1°C to 0.5°C for the near-term and by 0.2°C to 0.6°C for mid-century. Under RCP 8.5, the ensemble-mean maximum daily temperature for the spring-summer season increased by 1.3°C to 1.6°C for the near-term and by 1.9°C to 3.0°C for mid-century, while for the summer-autumn season it increased by 1.7°C to 2.1°C for the near-term and by 2.4°C to 3.5°C for mid-century. For the winter-spring season, the ensemble-mean maximum daily temperature increased by 0.2°C to 0.6°C for the near-term and by 1.0°C to 2.0°C for mid-century.

Under RCP 4.5, the ensemble-mean minimum daily temperature for the spring-summer season increased by 1.3°C to 1.6°C for the near-term and 1.7°C to 2.4°C for mid-century, while for the summer-autumn season it increased by 1.2°C to 1.9°C for the near-term and by 1.7°C to 2.8°C for mid-century. For the winter-spring season, the ensemble-mean minimum temperature increased by 0.1°C to 0.4°C for the near-term and by 0.4°C to 1.4°C for mid-century. Under RCP 8.5, the ensemble-mean maximum daily temperature for the spring-summer season increased by 1.3°C to 1.7°C for the near-term and by 1.9°C to 3.0°C for mid-century,

Table 6. Calibration and evaluation of the cultivars TCS10 and CAP. Calibration was performed with two treatments from different experiments. Evaluation was conducted with treatments that were not used for calibration.

	TCS10				CAP			
Variables	Observed	Simulated	RMSE	NRMSE	Observed	Simulated	RMSE	NRMSE
Calibration								
Anthesis (days)	80	80	0.7	1%	78	78	5.523	7%
Maturity (days)	108	108	1.0	1%	108	107	4.123	4%
Yield (kg ha^{-1})	5520	5712	193.4	2.2%	5768	6114	505.8	9%
Evaluation								
Anthesis (days)	81	80	1	1%	80	80	1	1%
Maturity (days)	106	106	1	1%	107	108	1	1%
Yield (kg ha^{-1})	6375	6519	144	2%	7974	8184	210	3%

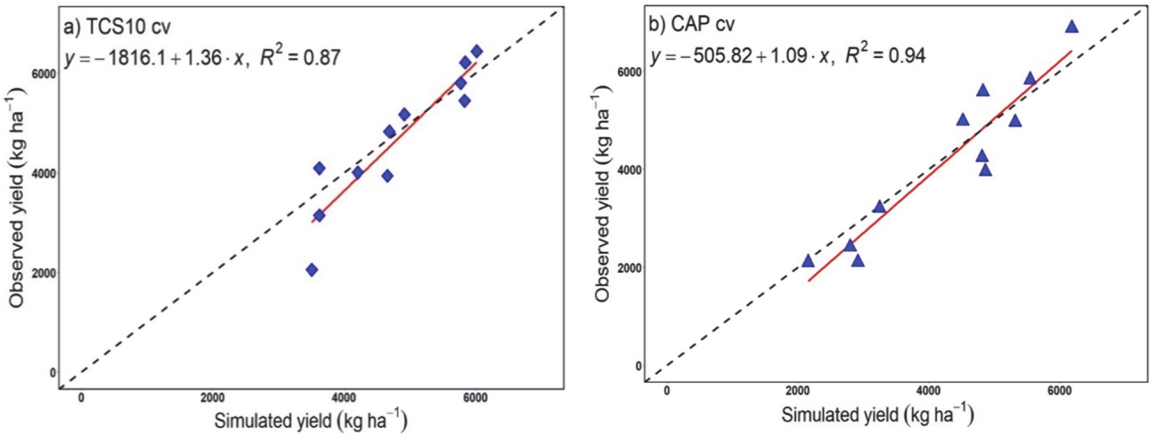

Figure 2. Relationship between simulated and observed grain yield for cultivars (a) TCS10 and (b) CAP during model evaluation. Observed data were collected in experimental trials conducted in the Artibonite Valley of Haiti in 2012, 2014, 2015, and 2016 by the Haitian Ministry of Agriculture. These data were not used for model calibration. Dashed lines are the 1:1 line, and solid red lines are the regression line.

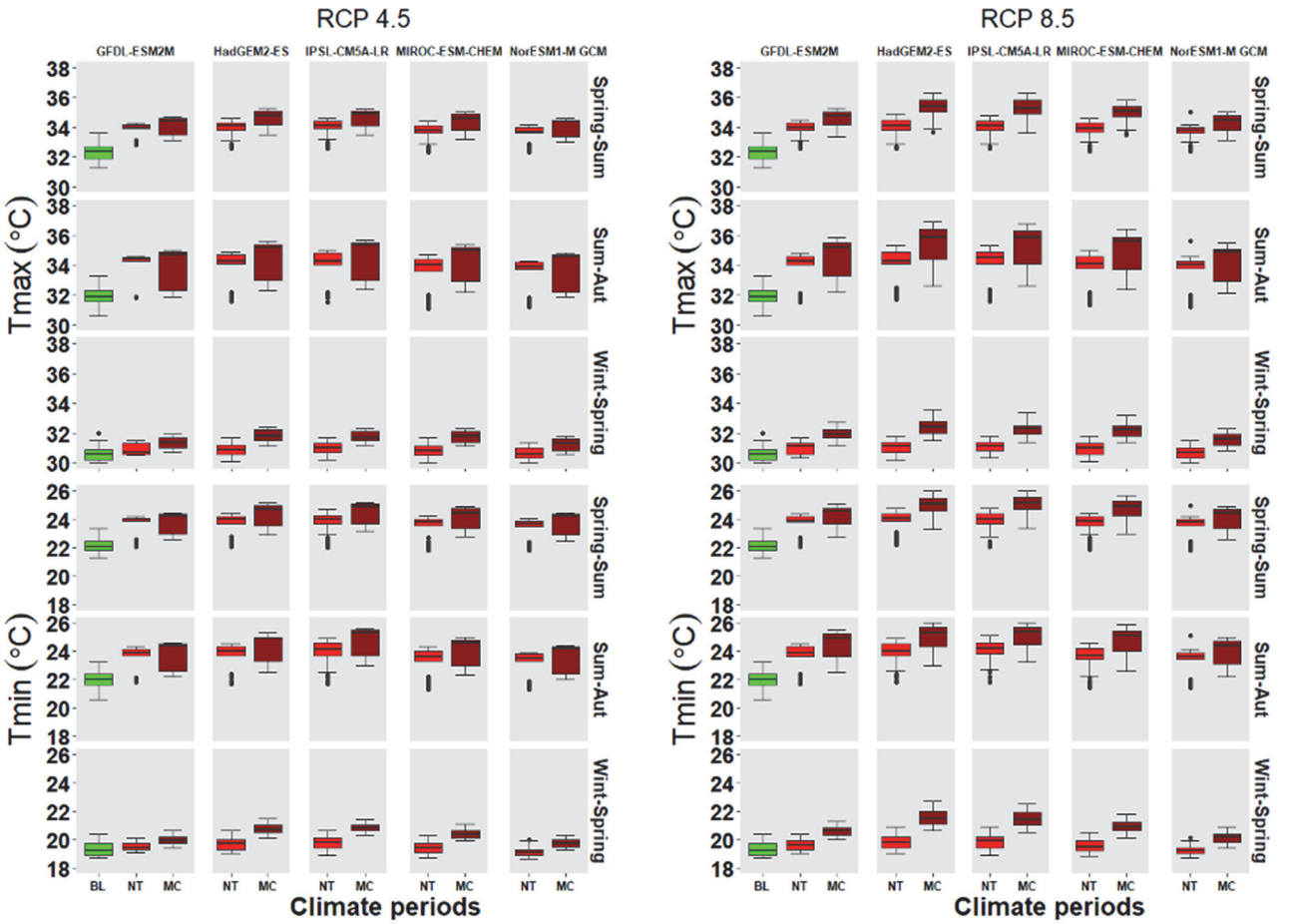

Figure 3. Projected variations of maximum and minimum temperature for five GCMs during three seasons (spring-summer, summer-autumn, and winter-spring) for two future climate periods (near-term: 2010-2039; and mid-century: 2040-2069) under RCP 4.5 and RCP 8.5 compared with the baseline. The fives GCMs are on the top *x*-axis, and the three seasons are on the right *y*-axis. The green, red, and dark red colors indicate the baseline (BL), near-term (NT), and mid-century (MC) climate periods, respectively.

while for the summer-autumn season it increased by 1.3°C to 1.9°C for the near-term and by 2.1°C to 3.4°C for mid-century. For the winter-spring season, the ensemble-mean maximum daily temperature increased by 0.2°C to 0.5°C for the near-term and by 0.8°C to 2.2°C for mid-century.

Solar radiation for all five GCMs under RCP 4.5 and RCP 8.5 decreased for the spring-summer season and increased for the summer-autumn and winter-spring seasons. Under RCP 4.5, the ensemble-mean solar radiation during the spring-summer season decreased by 0.9 to 1.0 MJ m^{-2} d^{-1} for the near-term and by 0.4 to 0.6 MJ m^{-2} d^{-1} for mid-century, while for the summer-autumn season it increased by 1.9 to 2.4 MJ m^{-2} d^{-1} for the near-term and by 1.8 to 2.3 MJ m^{-2} d^{-1} for mid-century. For the winter-spring season, the ensemble-mean solar radiation increased by 0.4 to 0.7 MJ m^{-2} d^{-1} for the near-term and by 0.3 to 0.8 MJ m^{-2} d^{-1} for mid-century. Under RCP 8.5, the ensemble-mean solar radiation during the spring-summer season decreased by 0.8 to 1.1 MJ m^{-2} d^{-1} for the near-term and by 0.2 to 0.7 MJ m^{-2} d^{-1} for mid-century, while in the summer-autumn season it increased by 2.0 to 2.3 MJ m^{-2} d^{-1} for the near-term and by 1.8 to 2.4 MJ m^{-2} d^{-1} for mid-century. For the winter-spring season, the ensemble-mean solar radiation increased by 0.6 to 0.8 MJ m^{-2} d^{-1} for the near-term and by 0.3 to 0.8 MJ m^{-2} d^{-1} for mid-century (fig. 4).

Rainfall was predicted to decrease for two of the three seasons with the five GCMs under both RCP 4.5 and RCP 8.5. Under RCP 4.5, the ensemble-mean rainfall in the spring-summer season increased by 30 to 114 mm for the near-term and by 19 to 104 mm for mid-century, while for the summer-autumn season it decreased by 61 to 89 mm for the near-term and by 13 to 39 mm for mid-century. For the winter-spring season, the ensemble-mean rainfall decreased by 38 to 85 mm for the near-term and by 12 to 28 mm for mid-century. Under RCP 8.5, the ensemble-mean rainfall in the spring-summer season increased by 60 to 83 mm for the near-term and by 44 to 106 mm for mid-century, while in the summer-autumn season it decreased by 63 to 93 mm for the near-term and by 35 to 110 mm for mid-century. For the winter-spring season, the ensemble-mean rainfall decreased by 14 to 23 mm for the near-term and by 7 to 44 mm for mid-century (fig. 4).

Simulation of Climate Change Impact on Rice Production

The simulation results showed a decrease in the number of days to flowering and maturity for both cultivars in the future climate periods compared to the baseline. Rice yield was predicted to increase for the winter-spring season, while

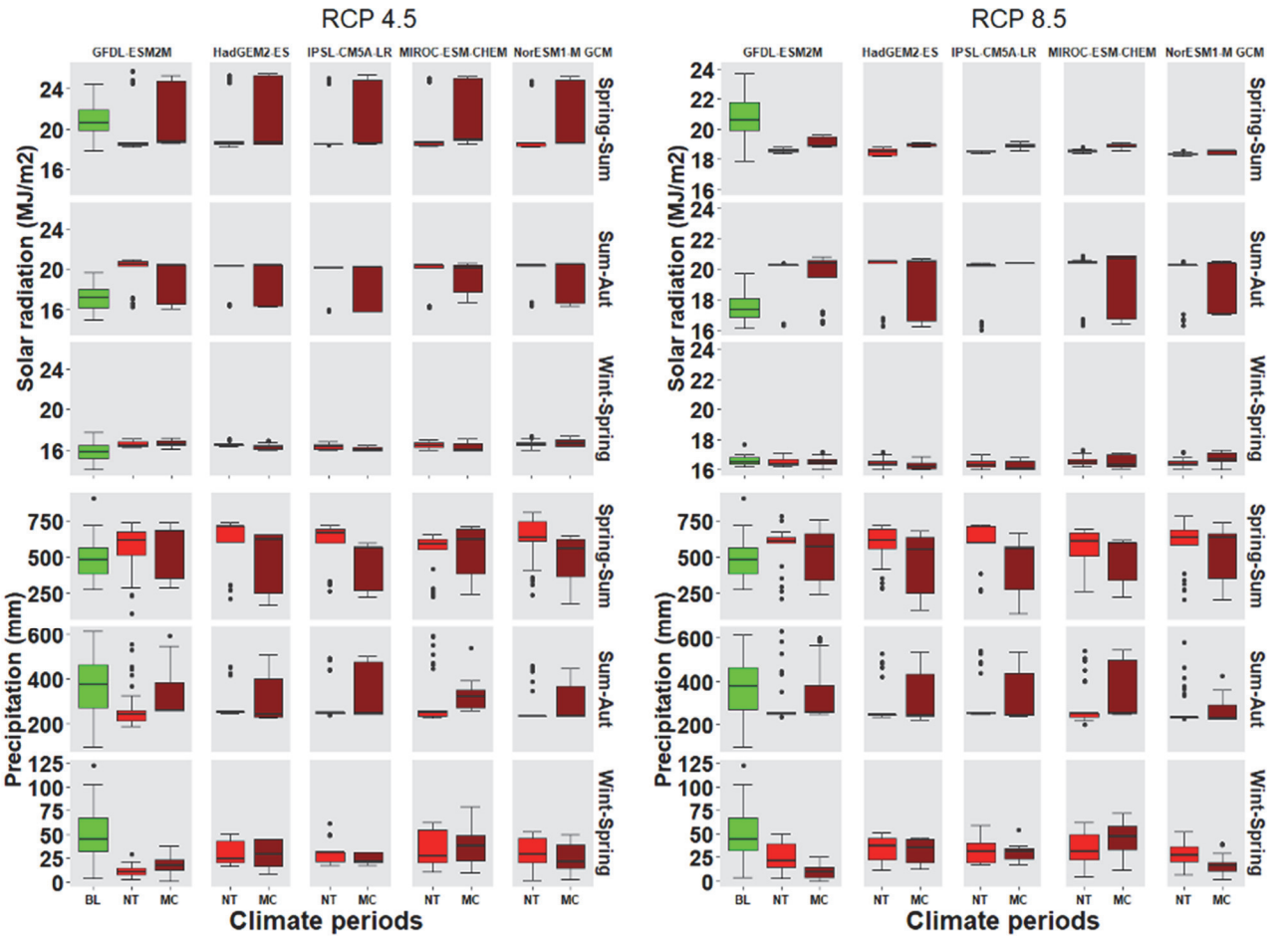

Figure 4. Projected variations in solar radiation and rainfall for five GCMs for three rice growing seasons (spring-summer, summer-autumn, and winter-spring) for two future climate periods (near-term: 2010-2039; and mid-century: 2040-2069) under RCP 4.5 and RCP 8.5 compared with the baseline. The green, red, and dark red colors indicate the baseline (BL), near-term (NT), and mid-century (MC) climate periods, respectively.

it was predicted to decrease for the spring-summer and summer-autumn seasons.

Climate Effects on Phenology of TCS10

According to the simulation results, the duration from planting to flowering date for cultivar TCS10 decreased under both RCPs (4.5 and 8.5) compared to the baseline. Under RCP 4.5, the ensemble-mean duration to flowering for the spring-summer season decreased by 4.5 to 5.5 days for the near-term and by 6.1 to 7.8 days for mid-century, while for the summer-autumn season it decreased by 3.6 to 4.7 days for the near-term and by 4.5 to 6.5 days for mid-century. For the winter-spring season, the ensemble-mean duration to flowering decreased by 0.5 to 1.6 days for the near-term and by 2.3 to 5.3 days for mid-century. Under RCP 8.5, the ensemble-mean duration to flowering for the spring-summer season decreased by 4.7 to 5.7 days for the near-term and by 6.8 to 9.2 days for mid-century, while for the summer-autumn it decreased by 3.8 to 4.8 days for the near-term and by 1.0 to 1.9 days for mid-century. For the winter-spring season, the ensemble-mean duration to flowering decreased by 5.4 to 7.6 days for the near-term and by 3.7 to 7.9 days for mid-century (fig. 5).

The duration from planting to physiological maturity also decreased for all future climate periods and all five GCMs and climate scenarios. Under RCP 4.5, the ensemble-mean duration to maturity for the spring-summer season decreased by 5.2 to 6.7 days for the near-term and by 7.4 to 9.5 days for mid-century, while for the summer-autumn season it decreased by 6.2 to 8.2 days for the near-term and by 8.3 to 10.8 days for mid-century. For the winter-spring season, the ensemble-mean duration to maturity decreased by 0.3 to 3.0 days for the near-term and by 3.7 to 7.8 days for mid-century. Under RCP 8.5, the ensemble-mean duration to maturity for the spring-summer season decreased by 5.4 to 6.8 days for the near-term and by 8.0 to 11.4 days for mid-century, while for the summer-autumn season it decreased by 6.8 to 8.6 days for the near-term and by 9.2 to 12.4 days for mid-century. For the winter-spring season, the ensemble-mean duration to maturity decreased by 0.6 to 3.4 days for the near-term and by 5.8 to 11.0 days for mid-century (fig. 5).

Climate Effects on Phenology of CAP

The duration from planting to flowering for the CAP cultivar was predicted to decrease under both RCP 4.5 and RCP 8.5 as compared to the baseline. Under RCP 4.5, the ensemble-mean duration to flowering for the spring-summer season decreased by 4.6 to 5.7 days for the near-term and by 6.1

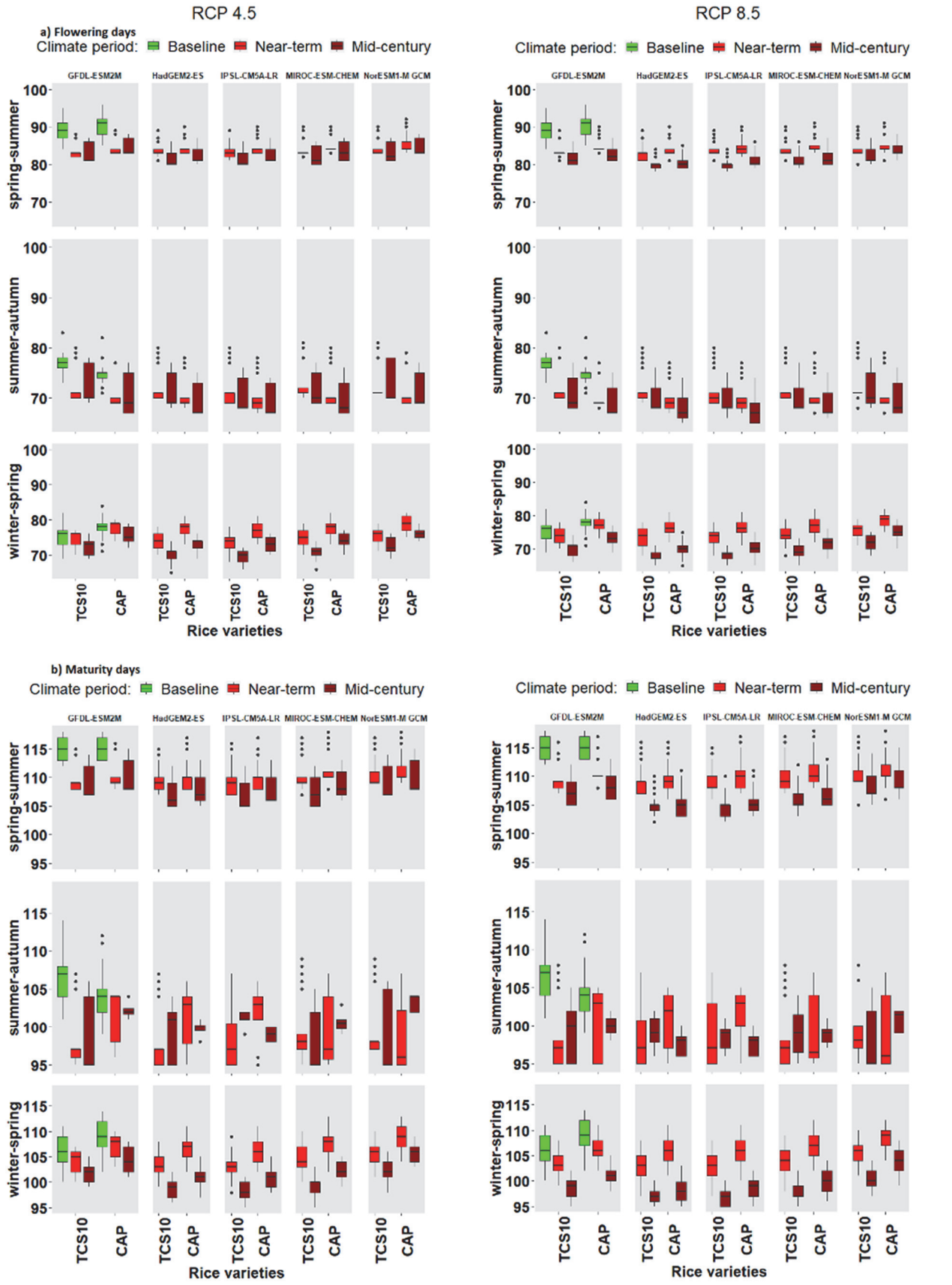

Figure 5. Predicted changes in (a) duration to flowering and (b) duration to physiological maturity for two future climate periods (near-term and mid-century) under two RCPs (4.5 and 8.5) for three rice growing seasons (spring-summer, summer-autumn, and winter-spring). The flowering and maturity days for each of the three seasons are on the left *y*-axis, the cultivars are on the bottom *x*-axis, and the GCMs are on the top *y*-axis. The green, red, and dark red colors indicate the baseline, near-term, and mid-century climate periods, respectively.

to 8.1 days for mid-century, while for the summer-autumn season it decreased by 3.2 to 4.4 days for the near-term and by 3.4 to 5.9 days for mid-century. For the winter-spring season, the ensemble-mean duration to flowering decreased by 0.2 to 1.2 days for the near-term and by 1.8 to 5.0 days for mid-century. Under RCP 8.5, the ensemble-mean duration to flowering for the spring-summer season decreased by 5.0 to 5.9 days for the near-term and by 6.7 to 9.4 days for mid-century, while for the summer-autumn season it decreased by 3.4 to 4.7 days for the near-term and by 5.0 to 7.1 days for mid-century. For the winter-spring season, the ensemble-mean duration to flowering decreased by 0.9 to 1.7 days for the near-term and 3.3 to 8.0 days for mid-century (fig. 5).

The duration to physiological maturity for the CAP cultivar decreased for the future climate periods with all the GCMs. Under RCP 4.5, the ensemble-mean duration to maturity for the spring-summer season decreased by 5.3 to 6.8 days for the near-term and by 7.7 to 9.9 days for mid-century, while for the summer-autumn season it decreased by 6.1 to 8.1 days for the near-term and by 7.4 to 8.4 days for mid-century. For the winter-spring season, the ensemble-mean duration to maturity decreased by 0.2 to 2.7 days for the near-term and 3.4 to 7.7 days for mid-century. Under RCP 8.5, the ensemble-mean duration to maturity for the spring-summer season decreased by 5.8 to 7.3 days for the near-term and by 8.3 to 11.6 days for mid-century, while for the summer-autumn season it decreased by 6.6 to 8.2 days for the near-term and by 8.9 to 11.6 days for mid-century. For the winter-spring season, the ensemble-mean duration to maturity decreased by 0.4 to 3.1 days for the near-term and 5.3 to 11.2 days for mid-century (fig. 5).

Climate Effects on Rice Yield

The yield of cultivar TCS10 was predicted to decrease for the spring-summer and summer-autumn seasons and to increase for the winter-spring season for the two climate periods (near-term and mid-century) under both RCP 4.5 (fig. 6) and RCP 8.5 (fig. 7). Under RCP 4.5, the ensemble-mean yield for the spring-summer season decreased by 4.9% to 6.2% for the near-term and by 5.3% to 6.8% for mid-century, while for the summer-autumn season it decreased by 4.4% to 7.7% for the near-term and by 4.0% to 9.1% for mid-century. For the winter-spring season, the ensemble-mean yield increased by 2.3% to 4.4% for the near-term and by 1.6% to 4.1% for mid-century. Under RCP 8.5, the ensemble-mean yield for the spring-summer season decreased by 5.3% to 6.5% for the near-term and by 5.8% to 7.2% for mid-century, while for the summer-autumn season it decreased by 5.3% to 7.6% for the near-term and by 8.5% to 11.5% for mid-century. For the winter-spring season, the ensemble-mean yield increased by 2.0% to 4.4% for the near-term and by 0.0% to 4.8% for mid-century.

Rice yield for cultivar CAP was also predicted to decrease for the spring-summer and summer-autumn seasons and to increase for the winter-spring season under both RCP 4.5 (fig. 6) and RCP 8.5 (fig. 7). Under RCP 4.5, the ensemble-mean yield for the spring-summer season decreased by 4.9% to 6.2% for the near-term and by 4.7% to 6.5% for mid-century, while for the summer-autumn season it decreased by 3.4% to 6.4% for the near-term and by 3.6% to 7.3% for mid-century. For the winter-spring season, the ensemble-mean yield increased by 1.8% to 3.2% for the near-term and by

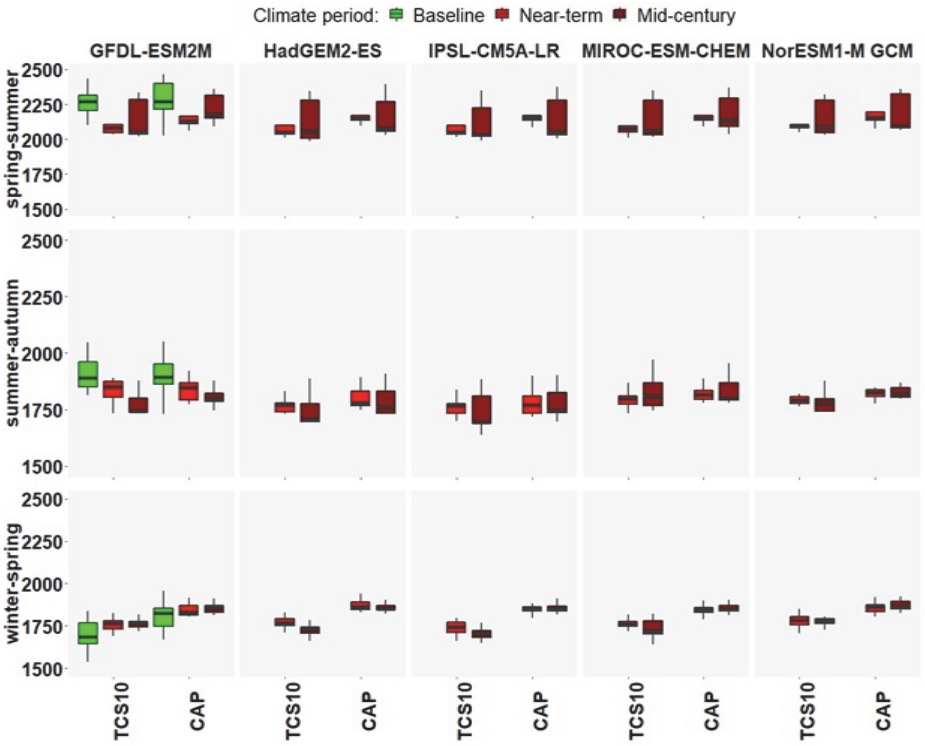

Figure 6. Simulated yields (kg ha^{-1}) of TCS10 and CAP rice cultivars for two climate periods (near-term and mid-century) during three growing seasons (spring-summer, summer-autumn, and winter-spring) with five GCMs in the Artibonite Valley under RCP 4.5 compared to the baseline. The cultivars (TCS10 and CAP) are on the bottom *x*-axis, the GCMs are on the top *x*-axis, and the yields for each of the three growing seasons are on the left *y*-axis. The green, red, and dark red colors indicate the baseline, near-term, and mid-century climate periods, respectively.

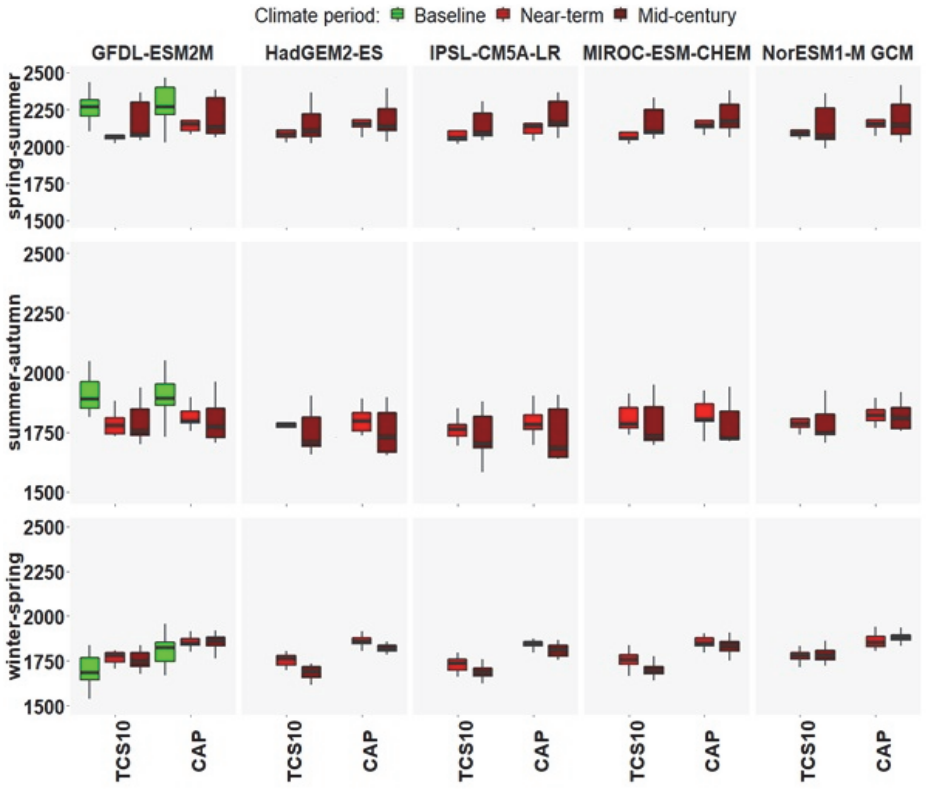

Figure 7. Simulated yields (kg ha^{-1}) of TCS10 and CAP rice cultivars for two climate periods (near-term and mid-century) during three growing seasons (spring-summer, summer-autumn, and winter-spring) with five GCMs in the Artibonite Valley under RCP 8.5 compared to the baseline. The cultivars (TCS10 and CAP) are on the bottom *x*-axis, the GCMs are on the top *x*-axis, and the yields for each of the three growing seasons are on the left *y*-axis. The green, red, and dark red colors indicate the baseline, near-term, and mid-century climate periods, respectively.

2.2% to 3.2% for mid-century. Under RCP 8.5, the ensemble-mean yield for the spring-summer season decreased by 4.4% to 5.5% for the near-term and by 4.6% to 5.6% for mid-century, while for the summer-autumn season it decreased by 4.0% to 6.1% for the near-term and by 4.7% to 11.2% for mid-century. For the winter-spring season, the ensemble-mean yield increased by 1.7% to 2.9% for the near-term and by 0.4% to 3.8% for mid-century.

Discussion

Model Performance

The quality of the data used in this study for model calibration and evaluation was considered intermediate according to the normal quality standards (Kersebaum et al., 2015). Information such as initial soil nitrogen was missing from the dataset; hence, assumptions were made to estimate the initial soil nitrogen concentrations based on soil data for the site and experimental rice yield data. However, information related to soil characteristics, management practices (such as the transplanting date and fertilizer application date and rate), and observations (including the anthesis and maturity dates and final yield) were sufficient to perform proper calibration and evaluation of the model according to the required minimum data set (Bao et al., 2017; Dos Santos et al., 2016).

The calibration and evaluation for rice phenology (flowering date and maturity date) and yield were adequate, although the field data set available for calibration and evaluation was relatively small, as only two treatments from two different experiments were used for calibration and one treatment from a different experiment was used for evaluation. The NRMSE values for phenology and yield for both cultivars were less than 10%, indicating good performance of the model. Similar NRMSE levels (<10%) were found in previous studies using CSM-CERES-Rice for prediction of duration to flowering, duration to physiological maturity, and grain yield (Basso et al., 2016; Li et al., 2016; Zhang et al., 2019).

Model Simulation

The number of days required for flowering and for physiological maturity was predicted to decrease with the two cultivars for the future climate periods and all seasons due to the increase in temperature. However, the reductions in time to anthesis and maturity were greater for CAP than for TCS10. When all three seasons were considered, the ensemble means for flowering and maturity were not significantly different for both cultivars. Although there have been no previous studies on the effect of climate change in the Artibonite Valley in Haiti, similar findings have been reported for other locations where climate change was predicted to result in a reduction in the number of days to anthesis and maturity due to an increase in temperature. For instance, Shi et al. (2015) found a decrease in the duration of the phenological phase due to higher temperatures using the RiceGrow model. Xu et al. (2017) reported similar conclusions using CSM-CERES-Rice for assessing climate change impacts on rice in the Sichuan basin in China.

During the winter-spring season, the increase in temperature triggered an increase in yield compared to the other two seasons. The average temperature during the winter-spring season did not exceed the optimal temperature range (14°C to 32°C) for yield in CSM-CERES-Rice (Lamsal et al., 2013). Rice is considered a heat-stress tolerant crop and has a higher optimal temperature for growth compared to temperate and sub-tropical cereal crops. In the tropics, the increase in local temperatures is usually smaller than the global mean temperature (Iizumi et al., 2017). Hence, the relatively low temperature during the winter-spring season for the future climate periods might benefit rice production in the Artibonite Valley.

The rice yields for both cultivars during the spring-summer and summer-autumn seasons were predicted to decrease due to warmer temperatures in the Artibonite Valley. Ritchie et al. (1998) stated that a reduction in the average growth duration due to temperature increasing beyond the optimal range could significantly affect rice yield. Net photosynthesis, which is the difference between gross photosynthesis and respiration, governs growth and is influenced by the temperature, and warm temperature could reduce grain size by increasing the rates of development and respiration (Hatfield et al., 2011). The warming climate could also trigger lower yield, spikelet sterility, and potential crop failure at extremely high temperatures, especially during the anthesis growth phase (Jagadish et al., 2015; Lobell and Gourdji, 2012). Thus, an increase in temperature close to very high temperatures during the rice growing seasons (spring-summer and summer-autumn in the Artibonite Valley) would reduce the rice growth rate by reducing the net photosynthesis. The growth duration, which includes the durations to flowering and maturity and determines the time for grain filling and biomass accumulation, was predicted to decrease under both RCPs (4.5 and 8.5) in a changing climate. Therefore, rice yields for both cultivars were expected to decrease. This finding is consistent with previous climate studies using a range of models (Bocchiola et al., 2015; Krishnan et al., 2007; Xu et al., 2017) that all predicted a reduction in rice yield.

The findings related to the effect of CO_2 agree with previous research that has been conducted with crop simulation models and in controlled experiments in growth chambers (Kontgis et al., 2019; Matsui et al., 1997; Zhao et al., 2019). However, the positive effects of CO_2 fertilization were insufficient to offset the adverse effects of rising temperatures on rice yield for the spring-summer and summer-autumn seasons in the Artibonite Valley. This is consistent with the findings of Kontgis et al. (2019) and Xu et al. (2017).

CONCLUSION

This study modeled the potential impacts of climate change on rice yield in the Artibonite Valley, which is the main region of rice production in Haiti. The impacts of the future climate for the near-term and mid-century under RCP 4.5 and RCP 8.5 were investigated using the CSM-CERES-Rice model. Rice yield was predicted to decrease for two of the three growing seasons (spring-summer and summer-autumn) for both RCPs (4.5 and 8.5), while the ensemble-mean yield for the winter-spring growing season was predicted to increase under RCP 4.5 and RCP 8.5 compared to the baseline. The results of this study suggest that adaptation strategies, such as changes in planting date, should be simulated to estimate each strategy's potential to reduce the negative effects of the changing climate on rice yield in the Artibonite Valley.

ACKNOWLEDGEMENTS

This study was supported by the SARD Feed the Future Project funded by USAID. Special thanks to Dr. Rose Koenig and the SARD project team in Haiti and in Gainesville, Florida. We also acknowledge the Haitian Ministry of Agriculture, Dr. Predner Duvivier, and Mr. Misdoing Lidelias for providing the experimental rice crop data and other data related to rice cultivation in the Artibonite Valley.

REFERENCES

Bai, J., Chen, X., Dobermann, A., Yang, H., Cassman, K. G., & Zhang, F. (2010). Evaluation of NASA satellite- and model-derived weather data for simulation of maize yield potential in China. *Agron. J., 102*(1), 9-16. https://doi.org/10.2134/agronj2009.0085

Bao, Y., Hoogenboom, G., McClendon, R., & Vellidis, G. (2017). A comparison of the performance of the CSM-CERES-Maize and EPIC models using maize variety trial data. *Agric. Syst., 150*, 109-119. https://doi.org/10.1016/j.agsy.2016.10.006

Basso, B., Liu, L., & Ritchie, J. T. (2016). A comprehensive review of the CERES-Wheat, -Maize, and -Rice models' performances. In D. L. Sparks (Ed.), *Advances in agronomy* (Vol. 136, pp. 27-132). Cambridge, MA: Academic Press. https://doi.org/10.1016/bs.agron.2015.11.004

Battisti, R., Bender, F. D., & Sentelhas, P. C. (2019). Assessment of different gridded weather data for soybean yield simulations in Brazil. *Theor. Appl. Climatol., 135*(1), 237-247. https://doi.org/10.1007/s00704-018-2383-y

Beven, K., & Binley, A. (1992). The future of distributed models: Model calibration and uncertainty prediction. *Hydrol. Proc., 6*(3), 279-298. https://doi.org/10.1002/hyp.3360060305

Bhattacharya, A. (2019). Chapter 1: Global climate change and its impact on agriculture. In A. Bhattacharya (Ed.), *Changing climate and resource use efficiency in plants* (pp. 1-50). Cambridge, MA: Academic Press. https://doi.org/10.1016/B978-0-12-816209-5.00001-5

Bocchiola, D. (2015). Impact of potential climate change on crop yield and water footprint of rice in the Po Valley of Italy. *Agric. Syst., 139*, 223-237. https://doi.org/10.1016/j.agsy.2015.07.009

Buddhaboon, C., Jintrawet, A., & Hoogenboom, G. (2018). Methodology to estimate rice genetic coefficients for the CSM-CERES-Rice model using GENCALC and GLUE genetic coefficient estimators. *J. Agric. Sci., 156*(4), 482-492. https://doi.org/10.1017/S0021859618000527

Challinor, A. J., Watson, J., Lobell, D. B., Howden, S. M., Smith, D. R., & Chhetri, N. (2014). A meta-analysis of crop yield under climate change and adaptation. *Nature Climate Change, 4*, 287-291. https://doi.org/10.1038/nclimate2153

Collins, W. J., Bellouin, N., Doutriaux-Boucher, M., Gedney, N., Hinton, T., Jones, C. D., ... Kim, J. (2008). Evaluation of HadGEM2 model. Technical Note 74. Exeter, UK: Meteorological Office Hadley Centre.

Dass, A., Nain, A. S., Sudhishri, S., & Chandra, S. (2012). Simulation of maturity duration and productivity of two rice

varieties under system of rice intensification using DSSAT v 4.5/CERES-Rice model. *J. Agrometeorol., 14*(1), 26-30.

Dixit, P. N., Telleria, R., Al Khatib, A. N., & Allouzi, S. F. (2018). Decadal analysis of impact of future climate on wheat production in dry Mediterranean environment: A case of Jordan. *Sci. Total Environ., 610-611*, 219-233. https://doi.org/10.1016/j.scitotenv.2017.07.270

Dos Santos, M. G., Faria, R. T., Palaretti, L. F., Dantas, G. D. F., Dalri, A. B., & Lopes, A. D. S. (2016). Calibration and testing of CS-CROPGRO model for common beans. *Engenharia Agricola, 36*(6), 1239-1249. https://doi.org/10.1590/1809-4430-eng.agric.v36n6p1239-1249/2016

Dufresne, J. L., Foujols, M. A., Denvil, S., Caubel, A., Marti, O., Aumont, O., ... Vuichard, N. (2013). Climate change projections using the IPSL-CM5 Earth System Model: From CMIP3 to CMIP5. *Climate Dyn., 40*(9), 2123-2165. https://doi.org/10.1007/s00382-012-1636-1

Dunne, J. P., John, J. G., Adcroft, A. J., Griffies, S. M., Hallberg, R. W., Shevliakova, E., ... Zadeh, N. (2012). GFDL's ESM2 g\Global coupled climate-carbon earth system models: Part I. Physical formulation and baseline simulation characteristics. *J. Climate, 25*(19), 6646-6665. https://doi.org/10.1175/jcli-d-11-00560.1

FEWS NET. (2018). Haiti staple food market fundamentals. Washington, DC: USAID Famine Early Warning System Network. Retrieved from https://reliefweb.int/report/haiti/haiti-staple-food-market-fundamentals-march-2018#:~:text=The%20main%20staple%20foods%20in,on%20supply%20and%20demand%20dynamics

Gao, Y., Wallach, D., Liu, B., Dingkuhn, M., Boote, K. J., Singh, U., ... Hoogenboom, G. (2020). Comparison of three calibration methods for modeling rice phenology. *Agric. Forest Meteorol., 280*, article 107785. https://doi.org/10.1016/j.agrformet.2019.107785

Guo, Y., Wu, W., Du, M., Liu, X., Wang, J., & Bryant, C. R. (2019). Modeling climate change impacts on rice growth and yield under global warming of 1.5°C and 2.0°C in the Pearl River delta, China. *Atmosphere, 10*(10), 567. https://doi.org/10.3390/atmos10100567

Hatfield, J. L., Boote, K. J., Kimball, B. A., Ziska, L. H., Izaurralde, R. C., Ort, D., ... Wolfe, D. (2011). Climate impacts on agriculture: Implications for crop production. *Agron. J., 103*(2), 351-370. https://doi.org/10.2134/agronj2010.0303

He, J., Jones, J. W., Graham, W. D., & Dukes, M. D. (2010). Influence of likelihood function choice for estimating crop model parameters using the generalized likelihood uncertainty estimation method. *Agric. Syst., 103*(5), 256-264. https://doi.org/10.1016/j.agsy.2010.01.006

Hoogenboom, G., Jones, J. W., Traore, P. C. S., & Boote, K. J. (2012). Experiments and data for model evaluation and application. In J. Kihara, D. Fatondji, J. W. Jones, G. Hoogenboom, R. Tabo, & A. Bationo (Eds.), *Improving soil fertility recommendations in Africa using the Decision Support System for Agrotechnology Transfer (DSSAT)* (pp. 9-18). Dordrecht, The Netherlands: Springer. https://doi.org/10.1007/978-94-007-2960-5_2

Hoogenboom, G., Porter, C. H., Shelia, V., Boote, K. J., Singh, U., White, J. W., ... Jones, J. W. (2018). Decision Support System for Agrotechnology Transfer (DSSAT). *4.7*. Gainesville, FL: DSSAT Foundation.

Hoogenboom, G., Porter, C., Boote, K., Shelia, V., Wilkens, P., Singh, U., ... Jones, J. (2019). The DSSAT crop modeling ecosystem. In *Advances in crop modeling for a sustainable agriculture* (pp. 173-216). Cambridge, UK: Burleigh Dodds Science Publishing. https://doi.org/10.19103/AS.2019.0061.10

Iizumi, T., Furuya, J., Shen, Z., Kim, W., Okada, M., Fujimori, S., ... Nishimori, M. (2017). Responses of crop yield growth to global temperature and socioeconomic changes. *Sci. Rep., 7*(1), 7800. https://doi.org/10.1038/s41598-017-08214-4

IPCC. (2014). *Climate Change 2014 - Impacts, Adaptation and Vulnerability: Part B: Regional Aspects*. Working Group II Contribution to the IPCC Fifth Assessment Report. Cambridge, UK: Cambridge University Press. https://doi.org/10.1017/CBO9781107415386

Iversen, T., Bentsen, M., Bethke, I., Debernard, J. B., Kirkevag, A., Seland, O., ... Sand, M. (2013). The Norwegian Earth System Model, NorESM1-M-Part 2: Climate response and scenario projections. *Geosci. Model Dev., 6*(2), 389-415. https://doi.org/10.5194/gmd-6-389-2013

Jagadish, S. V. K., Murty, M. V. R., & Quick, W. P. (2015). Rice responses to rising temperatures: Challenges, perspectives, and future directions. *Plant Cell Environ., 38*(9), 1686-1698. https://doi.org/10.1111/pce.12430

Jamieson, P. D., Porter, J. R., & Wilson, D. R. (1991). A test of the computer simulation model ARCWHEAT1 on wheat crops grown in New Zealand. *Field Crops Res., 27*(4), 337-350. https://doi.org/10.1016/0378-4290(91)90040-3

Jones, J. W., He, J., Boote, K. J., Wilkens, P., Porter, C. H., & Hu, Z. (2011). Estimating DSSAT cropping system cultivar-specific parameters using Bayesian techniques. In *Methods of introducing system models into agricultural research* (pp. 365-394). Madison, WI: ASA, CSSA, SSSA. https://doi.org/10.2134/advagricsystmodel2.c13

Jones, J. W., Hoogenboom, G., Porter, C. H., Boote, K. J., Batchelor, W. D., Hunt, L. A., ... Ritchie, J. T. (2003). The DSSAT cropping system model. *European J. Agron., 18*(3), 235-265. https://doi.org/10.1016/S1161-0301(02)00107-7

Jones, P. G., & Thornton, P. K. (2000). MarkSim: Software to generate daily weather data for Latin America and Africa. *Agron. J., 92*(3), 445-453. https://doi.org/10.2134/agronj2000.923445x

Kersebaum, K. C., Boote, K. J., Jorgenson, J. S., Nendel, C., Bindi, M., Fruhauf, C., ... Wegehenkel, M. (2015). Analysis and classification of data sets for calibration and validation of agro-ecosystem models. *Environ. Model. Softw., 72*, 402-417. https://doi.org/10.1016/j.envsoft.2015.05.009

Kontgis, C., Schneider, A., Ozdogan, M., Kucharik, C., Tri, V. P. D., Duc, N. H., & Schatz, J. (2019). Climate change impacts on rice productivity in the Mekong River delta. *Appl. Geogr., 102*, 71-83. https://doi.org/10.1016/j.apgeog.2018.12.004

Krishnan, P., Swain, D. K., Chandra Bhaskar, B., Nayak, S. K., & Dash, R. N. (2007). Impact of elevated CO_2 and temperature on rice yield and methods of adaptation as evaluated by crop simulation studies. *Agric. Ecosyst. Environ., 122*(2), 233-242. https://doi.org/10.1016/j.agee.2007.01.019

Lamsal, A., Amgai, L. P., & Giri, A. (2013). Modeling the sensitivity of CERES-Rice model: An experience of Nepal. *Agron. J. Nepal, 3*, 11-22. https://doi.org/10.3126/ajn.v3i0.8982

Lamy, J. D., Lofti, K., Louissaint, J, & Tescar, R. (2011). Effet de la fertilisation phosphatée et potassique sur le rendement de la variété de riz (*Oryza sativa*, L.) TCS10 à la vallée de l'Artibonite. Port-au-Prince, Haiti: Université d'Etat d'Haiti , Faculté d'Agronomie et de Medicine Vétérinaire.

Li, Y., Wu, W., Ge, Q., Zhou, Y., & Xu, C. (2016). Simulating climate change impacts and adaptive measures for rice cultivation in Hunan Province, China. *J. Appl. Meteorol. Climatol., 55*(6), 1359-1376. https://doi.org/10.1175/jamc-d-15-0213.1

Louissaint, J., & Duvivier, P. (2003). Rapport d'élaboration d'un référentiel technique fiable pour la fertilisation rationnelle et

économique des terres rizicoles de la vallée de l'Artibonite. Port-au-Prince, Haiti: Government of Haiti.
Maldonado, W., Valeriano, T. T. B., & de Souza Rolim, G. (2019). EVAPO: A smartphone application to estimate potential evapotranspiration using cloud gridded meteorological data from NASA POWER system. *Comput. Electron. Agric., 156*, 187-192. https://doi.org/10.1016/j.compag.2018.10.032
Matsui, T., Namuco, O. S., Ziska, L. H., & Horie, T. (1997). Effects of high temperature and CO_2 concentration on spikelet sterility in indica rice. *Field Crops Res., 51*(3), 213-219. https://doi.org/10.1016/S0378-4290(96)03451-X
ME. (2013). Deuxième communication nationale sur les changements climatiques. Port-au-Prince, Haiti: Ministère de l'Environnement. Retrieved from https://unfccc.int/sites/default/files/resource/htinc2.pdf
Pachauri, R. K., Allen, M. R., Barros, V. R., Broome, J., Cramer, W., Christ, R., ... van Ypserle, J.-P. (2014). Climate change 2014: Synthesis report. Contribution of Working Groups I, II, and III to the Fifth Assessment Report of the IPCC. Geneva, Switzerland: Intergovernmental Panel on Climate Change. Retrieved from http://epic.awi.de/37530/
Petersen, K. L. (2019). Impact of climate change on twenty-first century crop yields in the U.S. *Climate, 7*(3), 40. https://doi.org/10.3390/cli7030040
Pranuthi, G., & Tripathi, S. K. (2018). Assessing the climate change and its impact on rice yields of Haridwar district using PRECIS RCM data. *Climatic Change, 148*(1-2), 265-278. https://doi.org/10.1007/s10584-018-2176-4
Rankinen, K., Karvonen, T., & Butterfield, D. (2006). An application of the GLUE methodology for estimating the parameters of the INCA-N model. *Sci. Total Environ., 365*(1), 123-139. https://doi.org/10.1016/j.scitotenv.2006.02.034
Reilly, J., Tubiello, F., McCarl, B., Abler, D., Darwin, R., Fuglie, K., ... Rosenzweig, C. (2003). U.S. agriculture and climate change: New results. *Climatic Change, 57*(1), 43-67. https://doi.org/10.1023/A:1022103315424
Rinaldi, M., Losavio, N., & Flagella, Z. (2003). Evaluation and application of the OILCROP-SUN model for sunflower in southern Italy. *Agric. Syst., 78*(1), 17-30. https://doi.org/10.1016/S0308-521X(03)00030-1
Ritchie, J. T., Singh, U., Godwin, D. C., & Bowen, W. T. (1998). Cereal growth, development, and yield. In G. Y. Tsuji, G. Hoogenboom, & P. K. Thornton (Eds.), *Understanding options for agricultural production* (pp. 79-98). Dordrecht, The Netherlands: Springer. https://doi.org/10.1007/978-94-017-3624-4_5
Rosenzweig, C., Antle, J. M., Ruane, A. C., Jones, J. W., Hatfield, J. L., Boote, K. J., ... Mutter, C. Z. (2018). Protocols for AgMIP regional integrated assessments: Version 7.0. New ork, NY: Columbia University, Agricultural Model Intercomparison and Improvement Project (AgMIP). Retrieved from https://agmip.org/wp-content/uploads/2018/08/AgMIP-Protocols-for-Regional-Integrated-Assessment-v7-0-20180218-1-ilovepdf-compressed.pdf
Shi, P., Tang, L., Lin, C., Liu, L., Wang, H., Cao, W., & Zhu, Y. (2015). Modeling the effects of post-anthesis heat stress on rice phenology. *Field Crops Res., 177*, 26-36. https://doi.org/10.1016/j.fcr.2015.02.023
Singh, B., & Cohen, M. J. (2014). Climate change resilience: The case of Haiti. Nairobi, Kenya: Oxfam International. Retreived from https://www-cdn.oxfam.org/s3fs-public/file_attachments/rr-climate-change-resilience-haiti-260314-en_2.pdf
Singh, P. K., Singh, K. K., Baxla, A. K., Kumar, B., Bhan, S. C., & Rathore, L. S. (2014). Crop yield prediction using CERES-Rice vs 4.5 model for the climate variability of different agroclimatic zone of south and northwest plane zone of Bihar (India). *Mausam, 65*(4), 529-538.
Singh, P. K., Singh, K. K., Rathore, L. S., Baxla, A. K., Bhan, S. C., Gupta, A., ... Mall, R. K. (2016). Rice (*Oryza sativa* L.) yield gap using the CERES-Rice model of climate variability for different agroclimatic zones of India. *Curr. Sci., 110*(3), 405-413. https://doi.org/10.18520/cs/v110/i3/405-413
Stackhouse, P. W., Zhang, T., Westberg, D., Barnett, A. J., Bristow, T., Macpherson, B., & Hoell, J. M. (2018). POWER release 8 (with GIS applications) methodology. Hampton, VA: NASA Prediction of Worldwide Energy Resources (POWER) Project.
Sun, M., Zhang, X., Huo, Z., Feng, S., Huang, G., & Mao, X. (2016). Uncertainty and sensitivity assessments of an agricultural-hydrological model (RZWQM2) using the GLUE method. *J. Hydrol., 534*, 19-30. https://doi.org/10.1016/j.jhydrol.2015.12.045
Tiepolo, M., & Bacci, M. (2017). Tracking climate change vulnerability at municipal level in rural Haiti using open data. In M. Tiepolo, A. Pezzoli, & V. Tarchiani (Eds.), *Renewing local planning to face climate change in the tropics* (pp. 103-131). Cham, Switzerland: Springer International. https://doi.org/10.1007/978-3-319-59096-7_6
Tubiello, F. N., Rosenzweig, C., Goldberg, R. A., Jagtap, S., & Jones, J. W. (2002). Effects of climate change on U.S. crop production: Simulation results using two different GCM scenarios. Part I: wheat, potato, maize, and citrus. *Climate Res*, 20(3), 259-270. https://doi.org/10.3354/cr020259
USAID. (2011). Haiti climate change gender action plan (ccGAP) report. Washington, DC: USAID Climatelinks. Retrieved from https://www.climatelinks.org/resources/haiti-climate-change-gender-action-plan-ccgap-report
USAID. (2013). Haiti climate vulnerability profile. Washington, DC: USAID Climatelinks. Retrieved from https://www.climatelinks.org/resources/haiti-climate-vulnerability-profile
USAID. (2017). Climate risk profile: Haiti. Washington, DC: USAID Climatelinks. Retrieved from https://www.climatelinks.org/resources/climate-risk-profile-haiti
Vaghefi, N., Shamsudin, M. N., Radam, A., & Rahim, K. A. (2013). Modeling the impact of climate change on rice production: An overview. *J. Appl. Sci., 13*(24), 5649-5660. https://doi.org/10.3923/jas.2013.5649.5660
van Oort, P. A., & Zwart, S. J. (2017). Impacts of climate change on rice production in Africa and causes of simulated yield changes. *Global Change Biol., 24*(3), 1029-1045. https://doi.org/10.1111/gcb.13967
Warszawski, L., Frieler, K., Huber, V., Piontek, F., Serdeczny, O., & Schewe, J. (2014). The Inter-Sectoral Impact Model Intercomparison Project (ISI-MIP): Project framework. *Proc. Natl. Acad. Sci., 111*(9), 3228-3232. https://doi.org/10.1073/pnas.1312330110
Watanabe, S., Hajima, T., Sudo, K., Nagashima, T., Takemura, T., Okajima, H., ... Yokohata, T. (2011). MIROC-ESM 2010: Model description and basic results of CMIP5-20c3m experiments. *Geosci. Model Dev., 4*(4), 845-872.
White, J. W., Hoogenboom, G., Kimball, B. A., & Wall, G. W. (2011). Methodologies for simulating impacts of climate change on crop production. *Field Crops Res., 124*(3), 357-368. https://doi.org/10.1016/j.fcr.2011.07.001
White, J. W., Hoogenboom, G., Stackhouse, P. W., & Hoell, J. M. (2008). Evaluation of NASA satellite- and assimilation model-derived long-term daily temperature data over the continental U.S. *Agric. Forest Meteorol., 148*(10), 1574-1584. https://doi.org/10.1016/j.agrformet.2008.05.017
Wilcock, D. C., & Jean-Pierre, F. (2012). Haiti rice value chain assessment: Rapid diagnosis and implications for program

design. Boston, MA: Oxfam America. Retrieved from http://www. oxfamamerica.org/publications/haiti-rice-value-chain-research

Xiong, W., Holman, I., Conway, D., Lin, E., & Li, Y. (2008). A crop model cross-calibration for use in regional climate impacts studies. *Ecol. Model., 213*(3-4), 365-380. https://doi.org/10.1016/j.ecolmodel.2008.01.005

Xu, C.-C., Wu, W.-X., Ge, Q.-S., Zhou, Y., Lin, Y.-M., & Li, Y.-M. (2017). Simulating climate change impacts and potential adaptations on rice yields in the Sichuan basin, China. *Mitig. Adapt. Strat. Global Change, 22*(4), 565-594. https://doi.org/10.1007/s11027-015-9688-2

Yan, D., Zhu, Y., Wang, S., & Cao, W. (2006). A quantitative knowledge-based model for designing suitable growth dynamics in rice. *Plant Prod. Sci., 9*(2), 93-105. https://doi.org/10.1626/pps.9.93

Yang, J. M., Yang, J. Y., Liu, S., & Hoogenboom, G. (2014). An evaluation of the statistical methods for testing the performance of crop models with observed data. *Agric. Syst., 127*, 81-89. https://doi.org/10.1016/j.agsy.2014.01.008

Zhang, H., Zhou, G., Liu, D. L., Wang, B., Xiao, D., & He, L. (2019). Climate-associated rice yield change in the Northeast China Plain: A simulation analysis based on CMIP5 multi-model ensemble projection. *Sci. Total Environ., 666*, 126-138. https://doi.org/10.1016/j.scitotenv.2019.01.415

Zhao, X., Zhou, N., Lai, S., Frei, M., Wang, Y., & Yang, L. (2019). Elevated CO_2 improves lodging resistance of rice by changing physicochemical properties of the basal internodes. *Sci. Total Environ., 647*, 223-231. https://doi.org/10.1016/j.scitotenv.2018.07.431